Die approbierte Originalversion dieser Diplom-/Masterarbeit ist an der Hauptbibliothek der Technischen Universität Wien aufgestellt (http://www.ub.tuwien.ac.at).

The approved original version of this diploma or master thesis is available at the main library of the Vienna University of Technology (http://www.ub.tuwien.ac.at/englweb/).

Signature (Supervisor)

TECHNISCHE UNIVERSITÄT WIEN
Vienna University of Technology

Diploma Thesis

Test system design and measurements of the thermal conductivity for composite pipes

Carried out at the
Institute of Applied Physics

Author
Matthias Schafhauser, B.Sc.
Matr.nr. 0327659

Supervisor
Ao. Univ. Prof. Dr. Martin Gröschl

12.12.2012, Vienna

Signature (Author)

I would like to express my gratitude to the following persons for supporting this project:

Ao.Univ.Prof. Dipl.-Ing. Dr.techn. Martin Gröschl
(Vienna University of Technology -
Institute of Applied Physics - Sensors Group)

Mag. Katalin-Andrea Griessmair
(WKO Fachverband der Gas- und Wärmeversorgungsunternehmungen)

Dipl.-Ing. Dr. Josef Füreder
(Fa. Energie AG Oberösterreich Wärme GmbH)

Hr. Anton Steindl
(Fa. Isoplus Fernwärmetechnik GmbH)

Hr. Hermann Leutner
(Fa. Isoplus Fernwärmetechnik GmbH)

Dipl.-Ing. Gerald Moravi
(Fa. Steirische Gas-Wärme GmbH)

Amtsdir. Ing. Paul Berlinger, B.Sc.
(Vienna University of Technology -
Institute of Applied Physics - Electronics Workshop)

My family, girlfriend and friends for exercised patience and valuable advise.

Contents

1 Abstract **3**

2 Abstract (Deutsch) **4**

3 Introduction **5**

4 State of the Art **8**
4.1 Specifications 8
4.2 Measurements 9
4.3 Calculations 9

5 Theory **11**
5.1 Heat Conduction 11
5.2 Measurement Method 13
5.3 Interfering Factors 13
5.3.1 Outer Convection 13
5.3.2 Inner Convection 15
5.3.3 Heat Losses through Flanges 15
5.3.4 Contact Surfaces 15

6 Similar Research Studies **18**
6.1 Long-term thermal resistance of closed cell foam insulation 18
6.2 Konzeption und Aufbau eines Teststandes für thermische Vakuumröhrenabsorber 18
6.3 Alterung von Kunststoffmantelrohren 18

7 Measurement System **20**
7.1 Specimen Specifications 20
7.2 Hardware Components 20
7.2.1 Specimen Mounted Components 20
7.2.2 Specimen Enclosure 23
7.2.3 Control Components 24
7.2.4 Data Acquisition Components 27
7.3 Software Components 29
7.3.1 Arduino Code 29
7.3.2 Matlab Code 31
7.3.3 Finite element model 32

8 Measurements **36**
8.1 Reference Measurements 38
8.2 Deviations & Reproducibility 39
8.3 Result Overview 40
8.4 Interpretation 41

9 Conclusion **44**

List of Figures **46**

10 References **46**

1 Abstract

A significant fraction of human energy consumption is used for heating purposes thus efficient and durable insulation is a necessity. Although different materials have been used to insulate district heating pipes over the last decades only few studies have been conducted on the long-term aging effects.

This study has two main objectives: First, the development of a cost efficient and reliable measurement system to determine the thermal conductivity of insulation layers in compound pipes. Secondly, to analyze unused and used plastic jacket pipes in order to study the change of thermal conductivity due to aging effects in the insulation material for PUR closed-cell foams.

A variety of factors have to be considered in the design of a measurement system (e.g. the most suitable time constant, amount of available funds, sensor type, means of measuring surface temperatures, data acquisition layout and operation). The guidelines for such measurements given in appendix F of the European standard EN 253 and general literature have been researched and implemented as far as possible. The measurement system uses thermal equilibrium of the sample pipe with an ambient air volume and heating power monitoring to calculate the thermal conductivity of the insulation layer.

A small number of samples was chosen and more than 200 measurement runs conducted. The results indicate a smaller deterioration of the insulation properties than former studies with artificially aged pipes stated.

2 Abstract (Deutsch)

Ein signifikanter Anteil des menschlichen Energieverbrauches wird für Heizzwecke verwendet; daher ist effizientes und dauerhaftes Isolieren eine Notwendigkeit. Obwohl in den letzten Jahrzehnten verschiedene Materialien verwendet worden sind um Fernwärmerohre zu isolieren, gibt es nur wenige Studien die sich mit den Langzeiteffekten der Materialalterung beschäftigen.

Diese Arbeit hat zwei Hauptziele: Ein kosteneffizientes und verlässliches Messsystem für die Wärmeleitung in der Isolation von Fernwärmeverbundrohren zu entwickeln und anhand von natürlich gealterten Proberohren die Veränderungen des Wärmeleitwertes im Lauf der Verwendungsdauer zu bestimmen.

Eine Vielfalt von Faktoren wurden im Design des Messsystems berücksichtigt, wie zum Beispiel die Sensortypen, Datenerfassungsgestaltung und das vorhandene Budget. Die Richtlinien für solche Messungen, die in der zugehörigen Norm EN 253 und anderen Publikationen angegeben werden, sind in den Entwurf eingeflossen. Der Messaufbau verwendet thermisches Gleichgewicht der Probe mit der Umgebung und Heizenergieüberwachung um den Wärmeleitwert λ der Isolation zu berechnen.

Im Zuge dieser Arbeit wurde eine kompakte Stichprobe gewählt und mehr als 200 Einzelmessungen durchgeführt. Die Ergebnisse zeigen eine deutlich geringere Verschlechterung der isolierenden Eigenschaften als in bisherigen Studien, welche überwiegend künstlich gealterte Rohre verwendet, angegeben wurde.

3 Introduction

Minimizing energy losses in district heating systems is crucial for economic reasons and environmental protection. An example for the economic impact of the heat conductivity of the insulation material used in compound pipes is the following dilemma: a utility company can either choose higher investment costs due to a thicker insulation (this implies less lost heat energy but higher installation effort) or higher operation costs later on caused by a thinner pipe insulation. An environmental aspect of investigating the aging influence on thermal conductivity is the search for a pipe type with minimal degradation of this property over the known operation time.

In the last decades, a variety of different compound pipe types has been produced and is in use. These compound pipes consist of an inner pipe transporting the fluid, an insulation around it and an outer pipe to protect and improve the insulation. The typical choice of materials is steel for the inner pipe, high density Polyethylene (PEHD) or thin sheet steel (e.g. as folded spiral-seam pipe) for the mantle pipe and Polyurethan foam (PUR, made from the components Polyol and Isocyanate) as insulation layer. A change in this layer after a prolonged operation time can be visually detected and thus the question arises if there is a significant impact on the heat conduction properties of the compound pipe system. Fig.1 shows a pipe after more than 30 years of usage compared to a new one, documenting the change in color and structure of the foam after prolonged operation.

A great part of the existing publications and the standard procedure for quality testing of compound pipes are based on the assumption that the data generated with specimens which have been artificially aged by exposing them to high temperatures correlates in a trivial way with natural aging of the insulation material. In contrast to this procedure, the study at hand utilizes naturally aged specimens only to eliminate the uncertainties of the artificial aging process.

This thesis focuses on the development of a testing system for plastic jacket pipes and the change of thermal conductivity λ due to aging effects in the insulation

material. To gain representative sample pipe sections a detailed specimen specification defining the length, diameters and cell gas was issued. This simplifies the development of a suitable measurement system and ensures good comparability between different times of operation and mean operation temperatures. Determining which specimen has the smallest increase of λ regarding the duration of usage is an additional objective of this study. There are major challenges to overcome in order to achieve these aims:

- To calculate λ, the small heat transfer through the insulation material has to be measured. Therefore, a high measurement resolution is obligatory.
- The specimen has to be in a stationary thermal state. Thus, a temperature conditioned environment is necessary.
- A cost-conscious design and custom-build components are necessary to meet financial the restraints.
- Care has to be taken to generate a homogeneous sample. This is difficult as no artificial ageing techniques can be used.
- The necessary software to control the system, acquire and analyse the accumulated data has to be written.

Improved thermal insulation is the long-term objective of this study. The importance of this effort is highlighted if the potential energy savings are considered. To give an example 40 % to 50 % of the total energy consumed in Europe is used for buildings. The majority of it for heating purposes [1]. Although insulation materials can reduce the heat loss in buildings significantly, up to 50 % of the buildings in Europe are uninsulated [3]. Therefore, a knowledge of efficient insulation materials is increasingly valuable.

(a) New

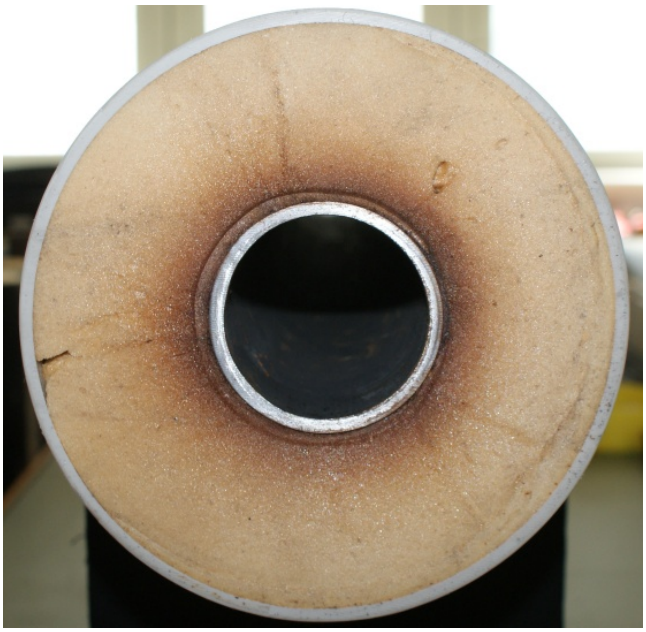

(b) Used (35 years of operation)

Figure 1: Plastic jacket pipe cross sections (DN50/160)

4 State of the Art

According to *T.E. Diller* [2], most heat-flux-measuring devices can be placed into one of four categories of methods:

(a) Thermal resistance measurement by sensing the temperature gradient and applying Fourier's law (Eq.3).

(b) Thermal capacitance method where a heat balance on the device yields the heat flux.

(c) Energy input or output method where heating or cooling energy is monitored.

(d) Measurement of the temperature gradient in an adjacent fluid.

The standard measurement method for the heat conductivity of pre-insulated pipes is described in appendix F of the European standard EN 253 [8, p.41ff] and corresponds to the first category, the current chapter shows the chosen design's deviations from this guideline and their reasons. If no difference is stated, the recommended methods were implemented as far as possible.

4.1 Specifications

The suggested specimen specifications are a nominal inner diameter of DN 50 [1] , an outer diameter of 125 mm and a length of 3 m. A reduced length of 1 m was determined in the design phase of this study to generate sufficient heat flux for the measurement. Due to the weight, heating and handling advantages, this shorter length is used. The diameters were verified with a slide gauge and a tape measure in the requested accuracy of ± 1 mm for lengths and ± 0.1 mm for diameters.

The measurement is meant to take place in still air at an ambient air temperature of 23 °C ± 2 °C. The caps sealing the specimen at the ends should be fitted with an auxiliary heating system or their heat flux should be calculated; the auxiliary heating system has to be build in an elaborately defined way with specially

[1] DN is the abbreviation of *Diameter Nominal* and is defined in the European standard EN 10255 [5] for medium weight steel pipes by the outer thread diameter of 2 inch. This results in a typical inner diameter of 53 mm.

insulated gaps. Choosing the second option, the heat flux was calculated in computer simulations and the air around the specimen was temperature controlled in a closed environment (insulated enclosure), thus fulfilling the requirement of air temperature changes below $\pm$ 1 °C during one measurement run.

4.2 Measurements

The surface temperature at the outside of the outer pipe and the inside of the inner pipe should be measured with four equally distributed sensors each (length- and diameter-wise). The accuracy for the temperature measurements are not to exceed an error of $\pm$ 0.3 °C. The temperature of the inner pipe surface should be in the interval 70 °C to 90 °C. To measure the inner temperature, the designed system is filled with a liquid and is heated axis-symmetrically with a sensor on each side measuring the fluid temperature. This value is assumed to be equal to the inner surface temperature due to the homogeneous medium, good insulation and small volume.

For integrating energy meters, a precision of 1.0 % is suggested within the minimum measurement time of 0.5 h per measurement. The energy meter used (ODIN Single) has accuracy class B $\hat{=}\pm$ 1 percent. The following quality criteria are given for the results: measurement runs have to be continued until the individual results of three subsequent tests with a pause of $\geq$ 0.5 h between them deviate by $\leq$ 1 1 % from the average of the results of these three tests and no one sided trend exists.

4.3 Calculations

The thermal conductivity at the mean temperature should be calculated using results for different inner pipe temperatures and linear regression. For type tests, the result should be expressed for a mean temperature of 50 °C and with a precision of 1×10^{-3} W/(m K). The thermal conductivities for the outer pipe and inner pipe materials is known: they are $\lambda_{PEHD} = 0.40$ W/(m K) for the outer pipe and $\lambda_{Steel} = 50$ W/(m K) for the inner pipe.

The equation to calculate the thermal conductivity of the insulation is given by Eq.1 according to the European standard EN 253 [8, p.45].

$$\lambda_{insulation} = \frac{ln\left(\frac{D_{c3}}{D_{s2}}\right)}{\frac{2\pi(T_1-T_4)L}{\Phi} - \frac{1}{\lambda_c}ln\left(\frac{D_{c4}}{D_{c3}}\right) - \frac{1}{\lambda_s}ln\left(\frac{D_{s2}}{D_{s1}}\right)} \tag{1}$$

5 Theory

5.1 Heat Conduction

The heat Q is the macroscopic description of the microscopic movement energy of molecules. It is defined in the first law of thermodynamics (Eq.2) where W is the work done by the system and ΔU is the difference in internal energy of the system.

$$Q = W + \Delta U \tag{2}$$

Its transfer does not require mass flow (similar to sound waves) and is described in Fourier's Law (Eq.3) where $\dot{Q}$ is the heat flux and $\frac{\partial T}{\partial x}$ the temperature gradient.

$$\dot{Q} = -\lambda \frac{\partial T}{\partial x}$$

or, simplified for isotropic materials

$$\dot{Q} = -\lambda \cdot \boldsymbol{\nabla} T \tag{3}$$

Eq.2 and Eq.3 are the basis for most instrumentation used to measure heat flux and transfer [13, p.16.59]. The thermal conductivity λ given in [W/(m K)] describes the amount of heat energy passing through a meter of a given material per Kelvin temperature difference between the two levels. It is a material dependent property and has to be measured individually for each material [6, p.18]. In the case of compound pipes the various layers have to be taken into account. A schematic drawing of such a pipe is shown in Fig.2.
A couple of calculation variants circulate for the problem at hand: in this study, the equation given in the ÖNORM EN 253 (Eq.1) [8, p.41] is modified to Eq.4 with an inner and outer diameter of the inner pipe d_{pi} and d_{po}, and, respectively, the mantle pipe d_{mi} and d_{mo}.

$$\lambda_{insulation} = \frac{ln\left(\frac{d_{mi}}{d_{po}}\right)}{\frac{2\pi L(T_{fluid}-T_{surface})}{\Phi} - \frac{1}{\lambda_{mantle}} ln\left(\frac{d_{mo}}{d_{mi}}\right) - \frac{1}{\lambda_{pipe}} ln\left(\frac{d_{po}}{d_{pi}}\right)} \tag{4}$$

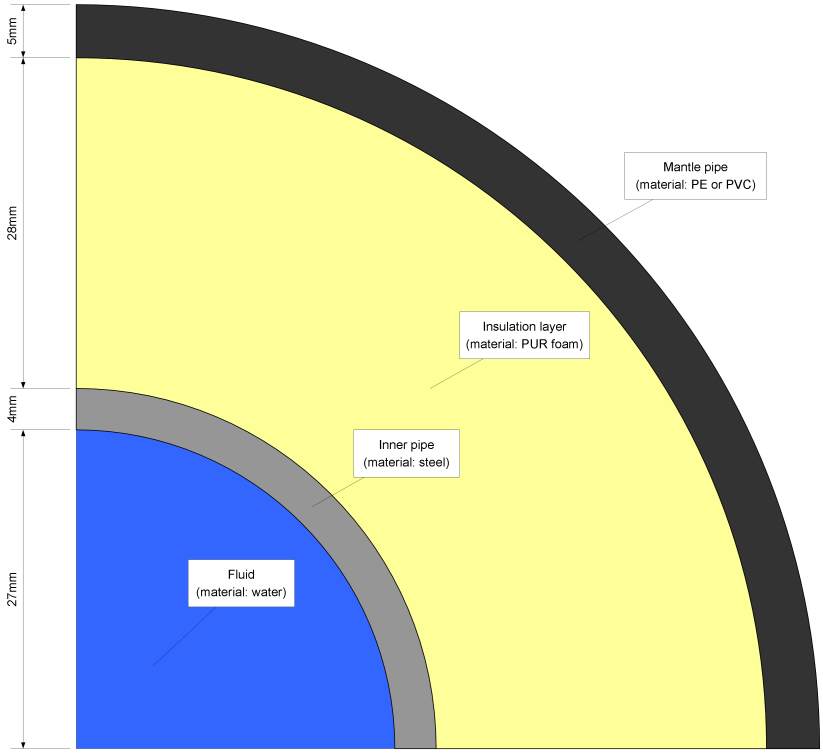

Figure 2: Schematic cross section of a DN 50-125 plastic jacket pipe

5.2 Measurement Method

Using a basic principle of thermodynamics, it is possible to determine λ with temperature and energy measurements.

> If two systems A and B, which are thermally uncoupled from the environment, are in thermal equilibrium with each other the heat fluxes $\dot{q}_{A\rightarrow B}$ and $\dot{q}_{B\rightarrow A}$ are equal.

In this case, the inner pipe is the higher temperature level and the ambient air around the outer mantle pipe is the lower level generating a heat flux. If the two temperature levels are kept stable, the energy fed into the inner pipe is equal to the energy flowing through the specimen material into the surrounding gas. Therefore, if an ohmic heater is used to replace the lost heat, the energy equation can be written as

$$P_{heating} = \dot{Q}_{in} = \dot{Q}_{out} = \dot{Q}_{loss}$$

5.3 Interfering Factors

The specimens are plastic jacket compound pipe pieces horizontally positioned within a temperature controlled, insulated housing. This geometric configuration has to be taken into account for the calculation of the heat flux Φ (or $\dot{Q}$) and the mean temperatures.

5.3.1 Outer Convection

The air in the housing is constantly moved by an air conditioning fan creating forced convection, whereas the measurement guideline EN 253 [8, p.41] assumes free convection. Therefore, the heat transfer coefficient α, which depends on several factors such as air flow speed and geometry [6, p.18], is different. This leads to a higher heat flux.
The fan used (EBM Pabst 12 W/230 V, 80x80x38 mm) has a maximal air flow of $50\,\mathrm{m}^3/\mathrm{h}$. This implies a maximal air flow speed of $u_{airflow} = \frac{V}{A} \cdot \frac{1}{t} = 2.17\,\mathrm{m/s}$. To determine the heat transfer coefficient α, the Nusselt number Nu_m was calculated

[11, p.392], [6, p.714], using the material dependant values of air $\rho, \lambda, Pr, \beta, \nu, \kappa$ at the reference temperature $T_* = 25\,°\mathrm{C}$ [6, p.172ff]. Solving the laminar and turbulent term in Eq.5 and using the mentioned material dependant properties, we can calculate Eq.6. Fig.3 depicts the solutions for varying temperature differences and air flow speeds.

$$Nu_m = 0,3 + \sqrt{Nu_{m,lam}^2 + Nu_{m,turb}^2} \tag{5}$$

$$Nu_{m,lam} = \frac{2}{\sqrt{\pi}}\sqrt{Re_x}\varphi_1(Pr)$$

$$\text{with } \varphi_1(Pr) = \frac{\sqrt{Pr}}{(1 + 1,973Pr^{0,272} + 21,29Pr)^{\frac{1}{6}}},$$

$$Nu_{m,turb} = \frac{0,037Re^{0,8}Pr}{1 + 2,443Re^{-0,1}(Pr^{\frac{2}{3}} - 1)}$$

$$Pr = \frac{\nu}{a} = \frac{\eta c_p}{\lambda} \rightarrow Pr_{air,25C} = 0,7068, \quad Re = \omega_m \frac{L}{\nu} = u\frac{a+b}{\nu}$$

$$\Rightarrow \text{heat transfer coefficient } \alpha = \frac{Nu_m \cdot \lambda}{L} = 9,94 \quad \frac{W}{m^2K} \tag{6}$$

In comparison to the heat transfer coefficient $\alpha = 154.0\,\mathrm{W/(m\,K)}$ for natural con-

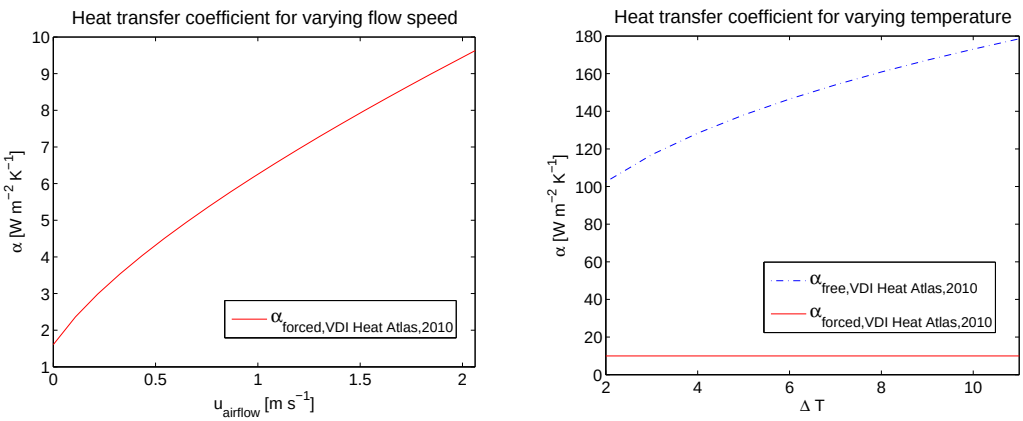

(a) Dependency of α_{forced} vs. air flow speed

(b) Dependency of α vs. ΔT

Figure 3: Plots concerning the heat transfer coefficient α

vection (in still air), this contribution can be omitted. An important assumption in ÖNORM EN 253 is heat transfer dominated by natural convection; therefore, Eq.4 is applicable for this design.

5.3.2 Inner Convection

The inner pipe is filled with water and heated by a cylindrical ohmic heating element along the center axis, thus generating free convection of the liquid. Furthermore, temperature lamination in the fluid must be small to gain representative results from the temperature sensors.
To approximate the occurring flow velocities and the temperature field within the compound pipe, a two dimensional finite element model was created. The resulting data shows two distinct aspects of the given geometry.
Fig.4 gives the free and constricted flow velocity fields after 10 min operation: the maximum velocities are small ($\leq 0.01\,\mathrm{m\,s^{-1}}$) and allow for nearly homogeneous temperature results in the fluid. Moreover, this data implicates a sufficiently fast mixing of the fluid as indicated by the asymmetric velocity distribution in Fig.4b.

Fig.5 focuses on the temperature distribution around the heating element in the center. The simulation shows a smooth and nearly perfect symmetrical temperature field at the outer surface. This supports the planned equidistant placement of the Pt-100 sensors around the whole diameter. According to Fig.5b, the placement of the sensor pipe in the upper half is feasible due to the insignificant shift in the temperature field caused by the constriction of the flow.

5.3.3 Heat Losses through Flanges

The heat flux through the two flanges at either side of the specimen must be known for the chosen measurement method. Using the finite element method (FEM), these values can be obtained by simulations (see chapter 7.3.3). For a desired fluid temperature of $T_{fluid} = 80\,°\mathrm{C}$ and an ambient air temperature of $T_{ambient} = 23\,°\mathrm{C}$, the calculated heat flux through both flanges adds up to $\dot{Q}_{flanges} \approx 18\,\mathrm{W}$. This information was used to correct the measurement data in the analysis software.

5.3.4 Contact Surfaces

Heat transfer in solids has to be considered regarding undesired heat losses: to minimize contact surfaces, the specimens were mounted on two supports. These structures are made from high density polyethylene with a v-shaped notch where

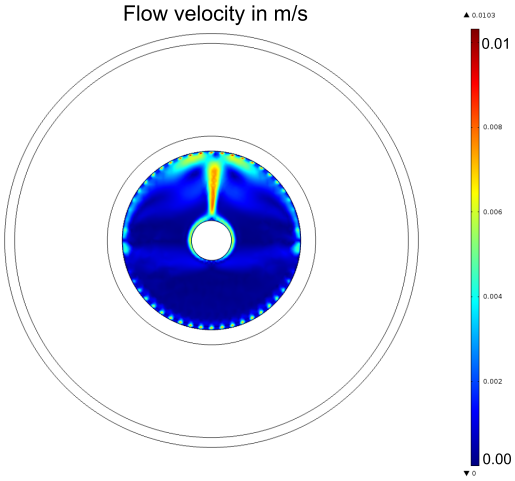

(a) Free field

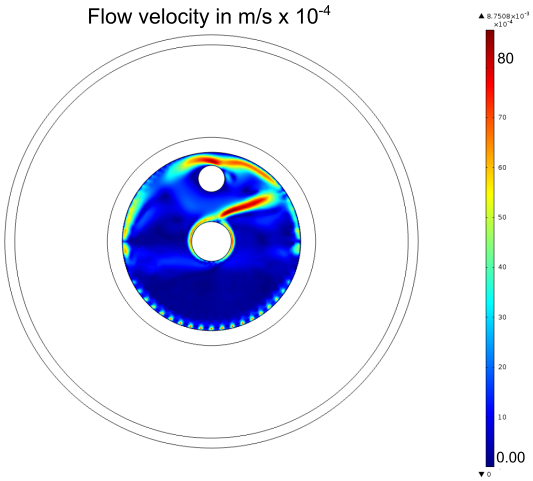

(b) Constriction due to sensor pipe

Figure 4: Simulation data of flow distribution in a compound pipe

the specimens are positioned. The losses due to heat transfer into the contacting materials is, however, insignificant because of the low heat conductivity of PEHD and the very small contact surfaces in the v notch. Furthermore, the collars fixing the sensors to the outer pipe surface have to be considered: they are made of stainless steel cut into narrow stripes. Due to their good heat conductivity and the small surface area they cover, no significant influence is to be expected.

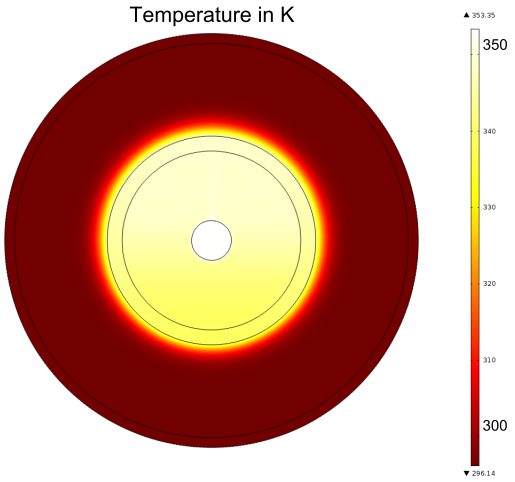

(a) Free field

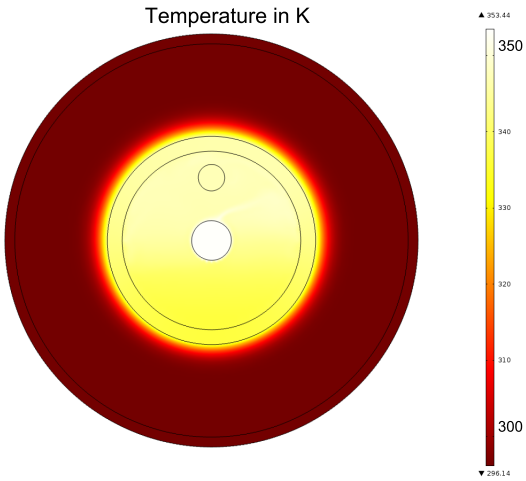

(b) Constriction due to sensor pipe

Figure 5: Simulation data of temperature distribution in a compound pipe

6 Similar Research Studies

6.1 Long-term thermal resistance of closed cell foam insulation [9]

The authors focus on the aging effects increasing the thermal conductivity of closed cell foam insulation materials. They conclude that diffusion of air into and blowing gas out of the foam cells is the main effect causing increased thermal conductivity. Furthermore, it is stated that the diffusion speed is very high at the beginning of the product lifetime and slows down with time.

6.2 Konzeption und Aufbau eines Teststandes für thermische Vakuumröhrenabsorber [4]

A project measuring the thermal losses of solar receivers is described. A heating rod is used to replace lost heat energy and to measure the heat flux when an equilibrium is reached. Heating coils and ceramic insulation caps (due to the high temperatures of $T \approx 320\,°\mathrm{C}$) are used to prevent axial heat losses at the ends. A one dimensional simulation model was created to compare the measurement data with a theoretical model. To increase sensor data accuracy, the temperature sensors were calibrated. Due to the tight space restrictions in the receiver pipe, a suitable mounting method for the sensors had to be developed.

6.3 Alterung von Kunststoffmantelrohren [10, p.11]

Only very few studies deal with the effects aging has on thermal conductance of closed cell foam insulation. Comparable data to the present study was presented in the ninth district heating colloquium in Dresden 2004, where the majority of specimens with operation durations up to 25 years have a thermal conductivity of below $\lambda = 0.032\,\mathrm{W/(m\,K)}$.

The authors conclude that air replacing the cell gas is the main mechanism leading to higher λ values caused by the higher heat conductivity of air compared to the typically used blowing gases. Furthermore, it is stated that approximately two

thirds of the thermal losses are dominated by the cell gas properties and therefore specimens were sealed with aluminium foil immediately after they were cut. In the conclusion, the authors declare the need to re-evaluate the usual method of high temperature aging of compound pipes ($T \geq 180\,°\mathrm{C}$) for long term property prediction.

7 Measurement System

A variety of factors have to be considered for a successful design of a measurement system, such as e.g. the most suitable time constant, amount of available funds, sensor type, means of measuring surface temperatures, data acquisition layout and operation. Many of these aspects for choosing a temperature measuring system are listed in the *Handbook of Heat Transfer* [13, p.16.55 f].

7.1 Specimen Specifications

The following specifications for the specimens were defined to simplify the mechanical design and comparability of results:

- Type of pipe: plastic jacket pipe
- Length : 1.00 m
- Nominal diameter : DN 50
- Outer diameter: $\leq$ 12.7 cm
- Pipe cut finish: straight, planar cut through all layers perpendicularly to the pipe axis. Inner edge deburred.
- Foaming agent : cyclopentan as reference; for other agents, multiple specimens of varying ages were asked for.

7.2 Hardware Components

7.2.1 Specimen Mounted Components

The specimens are capped by two circular flanges made from stainless steel (Type 4301, $\lambda = 15\,\mathrm{W/(m\,K)}$, [12]) with an EPDM rubber sealing ring fastened by four thread bars. Both sides are identically designed. Fig.6 shows the technical drawing. On one side an ohmic heating element with $P_{max} = 1\,\mathrm{kW}$ and $T_{max} = 95\,°\mathrm{C}$ is screwed into the flange along the center axis. On the other side a pressure relief valve with $p_{release} = 1\,\mathrm{MPa}$ is mounted to remove surplus fluid in the warm-up

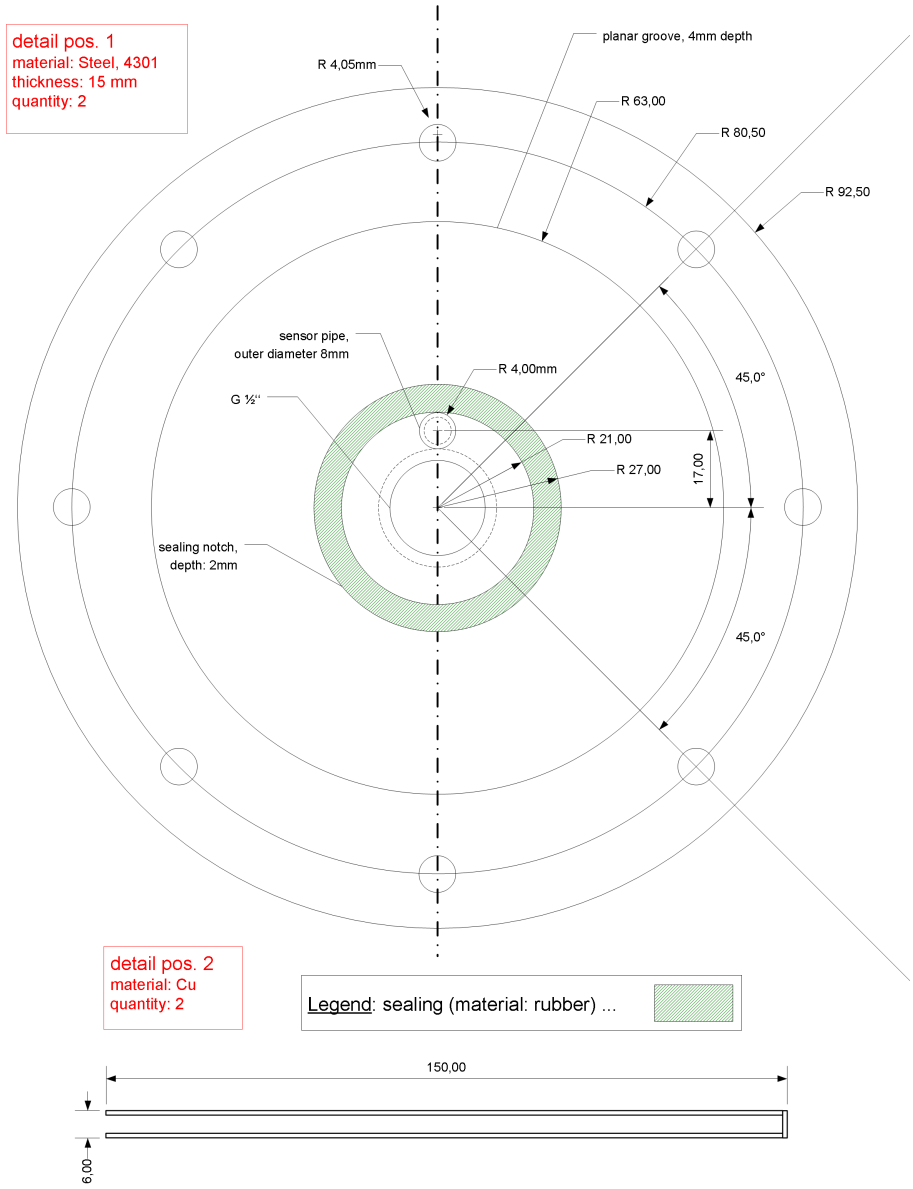

Figure 6: Technical drawing of Flange A

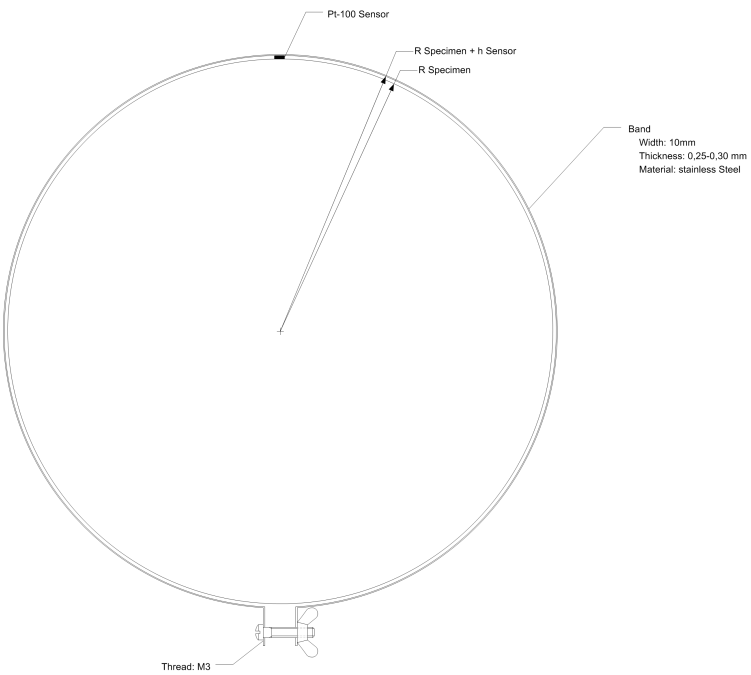

Figure 7: Stainless steel bands for sensor mounting

phase and to act as an automatic fail safe. At each flange a copper pipe with an outer diameter of 8.00 mm protects the Pt-100 sensors measuring the fluid temperature inside the specimen. Planar grooves on the inner side of the flanges ease the necessary alignment for pressure tightness. Outer specimen diameters up to 160 mm can be accommodated. To minimize heat losses at the flanges two types of insulation were used: insulating caps made from polyurethane foam with a thickness of more than 60 mm on the sides and more than 120 mm at the outer side. And an EPDM rubber ring for the inner sides of the flanges protruding the outer specimen diameter with a material thickness of 4 mm.

The Pt-100 sensors measuring the outer surface temperature of the specimen are fixed with four thin sheet steel collars. Stainless steel in a thickness of 0.8 mm and width of 10 mm was chosen for the collars because of the potentially wet surroundings and the relatively small minimum bending radius of $\approx$ 62.5 mm. For each outer diameter four pieces are needed, Fig.7 shows a simplified technical drawing of these elements.

Two specimen supports with a v-shaped notch are used to position the specimen in the enclosure. The notch shape and the material (PEHD slates with 10 mm thickness) were chosen to minimize heat flow through contact surfaces.

7.2.2 Specimen Enclosure

(a) Basis enclosure

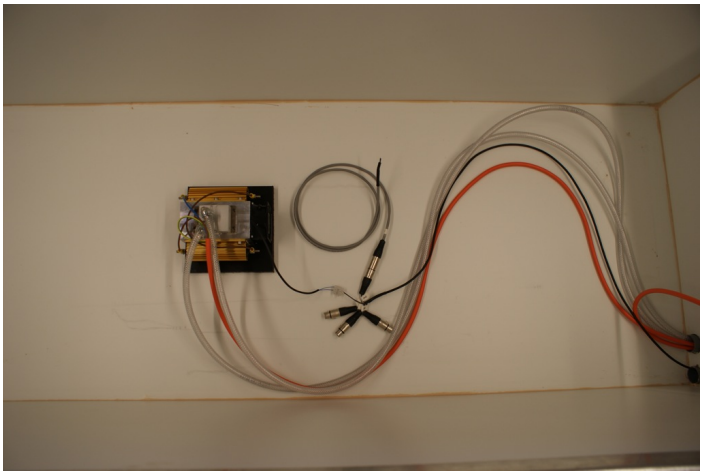

(b) Enclosure with heating / cooling block

Figure 8: Specimen housing

The specimen enclosure was build from insulation panels consisting of three layers: two thin sheet metal plates and a hard foam insulation in between. Rectangular frames made of sheet steel bended and welded form the structural parts with the panels fastened to them with rivets.

The enclosure was designed for the main tasks of keeping the air around the specimen thermally insulated from the surrounding air and to prevent undesired air flow. Therefore, additional sealing of the inner edges with silicone compound and a hollow rubber insulation profile was added for the lid.

Two feedthroughs made from DN 40 HT sewage pipes were installed to allow easy access into the housing for necessary cables and tubes. A set of four rotatable casters have been added for transport. To condition the air temperature in the

Figure 9: Specimen enclosure top view with mounted sample

enclosure a heating and cooling block was added. It consists of two heating resistors and a fluid heat sink mounted on a common string heat sink. Air is blown through the fins of the common heat sink with a fan.

Fig.9 shows a top view of a fully assembled sample in the specimen enclosure ready for measurement.

7.2.3 Control Components

A 19 inch industrial standard housing with 3 rack units height holds the control components. A three phase mains connection is used to reduce electromagnetic noise in the whole system (e.g. caused by valves, relays and motors). In the back section a DIN cap rail is installed for the various power distribution elements and a 12 V power supply for the electronic circuits. Self locking connectors were used

(a) Front view

(b) Top view

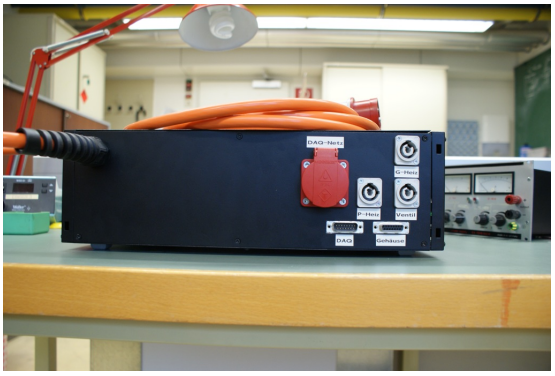

(c) Back view

Figure 10: Finished Control Unit

for all critical power lines. An isolated ground receptacle was integrated for the data acquisition (DAQ) module mains supply. A 15 line multicore cable connects all necessary sensors and control lines with the specimen enclosure. An other multicore of the same dimension connects the control with the data acquisition unit.

A PID controller (RedLion, type: T48, Model T4821000) in combination with three solid state relays is used to regulate and monitor the air temperature in the specimen enclosure. One relay drives through an insulating transformer two heating resistors, an other one switches a magnetic valve which supplies the fluid heat sink with cooling water. A third relay supplies the fan of the heating and cooling block inside the specimen housing.

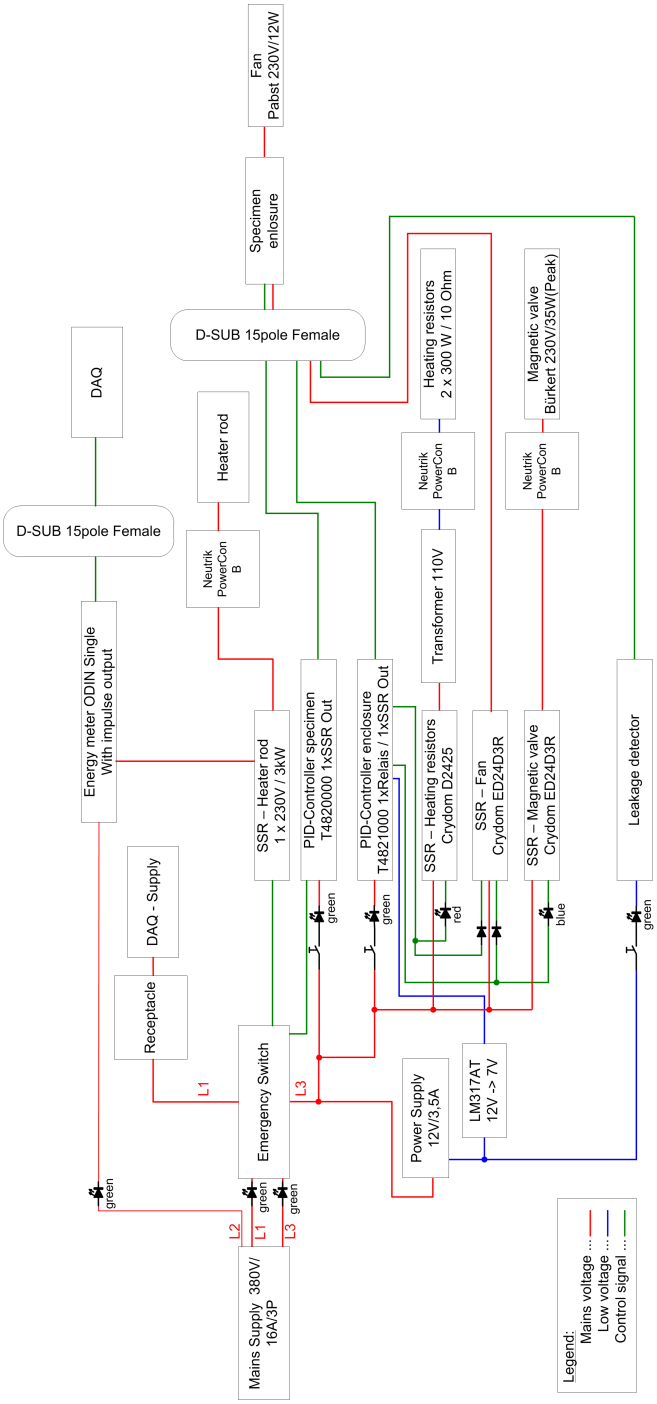

Figure 11: Block schematic of Control Unit

The second PID controller (RedLion, type: T48, Model T4820000) switches a solid state relay which is connected through the energy meter to the heating element inside the specimen to heat the fluid. The energy meter (ABB, type: OD1365) features a light emitting diode (LED) which sends a short light pulse for every 1 W h measured. This flash is detected via a light dependent resistor mounted in front of the red LED. After filtering the dark current it is sent to the data acquisition as digital input. To minimize electromagnetic noise in the transmitted signal the light pulse detector circuit is supplied by the DAQ 5.00 V reference source and outfitted with a RC-circuit.

A couple of necessary safety components were implemented in the design of the control unit. An emergency stop push-button disconnects all supply lines including the cooling water if activated. A temperature controlled fan keeps the various heat sinks of the electronic components cool if the temperature rises above an adjustable level. The power supplies of the PID controllers and the remaining circuits can be switched on individually. A leakage detection circuit with two red LED indicators shows if there is a spill in the specimen enclosure.

7.2.4 Data Acquisition Components

A 19 inch industrial standard housing with 2 rack units height holds the data acquisition components together with a switch-mode power supply delivering 12 V and 5 V to the other circuit boards. The reference voltage source was designed for an constant output of 5.00 V to ensure reliable measurements with a voltage regulator (type: LM317AT) as the core element.

Two sensor types were used in the system: Pt-100 resistive sensors and TC1047 temperature-to-voltage converter. All sensors are connected to the processing circuit board via shielded cables through a multicore cable with 36 lines. XLR connectors were chosen for the link between sensors and sensor multicore due to their rugged design. On the other end a Centronics connector is used which can be seen in Fig.12c.
On the preprocessing circuit board ten XTR105PA 4 mA to 20 mA current trans-

(a) Front view

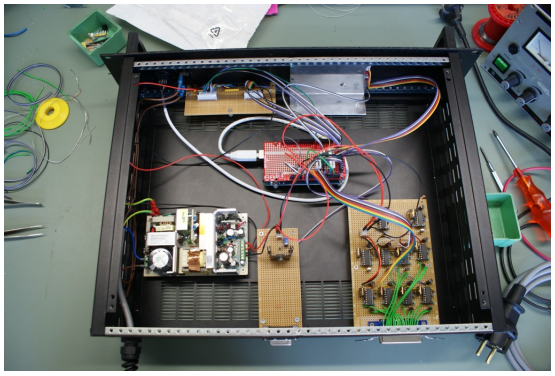

(b) Top view

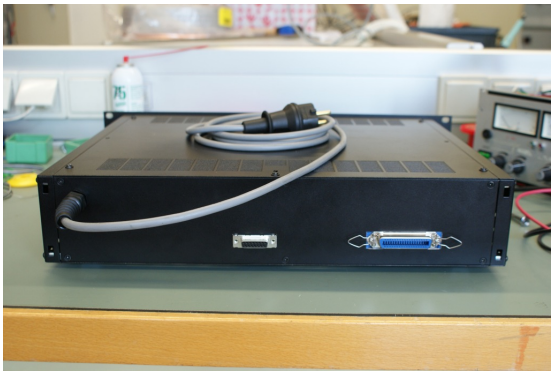

(c) Back view

Figure 12: Finished Data Acquisition Unit

mitter chips with integrated linearization for Pt-100 elements are mounted to convert the resistance differences to current differences. Those are transformed into a voltage signal by high accuracy resistors with low temperature drift. The current transmitter chips are specially designed for the use with resistance temperature sensors. An advantage of these transmitters is a broad band of possible supply voltages and decoupling from noise emitted by the power supply.

An Arduino Mega 2560 Revision 3 board is the heart of the data acquisition electronics (see Fig.12b). It features an Atmega2560 microcontroller with three serial ports, one serial via USB port, 16 analog inputs, 54 digital in- or outputs and 256 KB flash memory. For the data connection a robust USB receptacle in the front grants access to the microcontroller board via a virtual serial port. For good

usability a 16 by 2 characters LCD display, a rotary encoder, four push-buttons and a row of LEDs ($\varnothing = 3\,\mathrm{mm}$) were installed to choose and view sensor readings. The 10-bit analog to digital converter (ADC) of the Arduino board combined with the reference voltage source achieve a resolution of less than 0.5 mV per ADC step. This implies a resolution below 0.3 °C with an error of $\leq 1.1\,\%$ for the XTR105PA with Pt-100 circuits. Furthermore, less than 0.5 °C resolution with an accuracy of typical ± 0.5 °C (max.± 2 °C for $T \leq 85\,°\mathrm{C}$) for the TC1047A semiconductor sensors.

7.3 Software Components

7.3.1 Arduino Code

The first block of code defines and initializes a variety of configuration variables such as the data storage arrays, input and output ports and start values. Concerning the ports a specialty of microcontrollers called interrupt service routines (ISR) is used to read energy meter pulses and the rotary encoder status. These ISRs allow a certain port to interrupt the microprocessor in realtime to make sure the received input is processed immediately by a predefined function if a certain signal change is read.

A subsequent block initializes the serial data connection and deals with the LCD display settings. Following this first part of the program core functions are defined: the setup-function which is called only once at power up and the loop-function which is afterwards repeated infinitely. In the loop-function at first the readout routine for the XTR105PA channels and their serial output is executed followed by the LCD output and TC1047 channel readout routine.

We will now focus on the XTR105PA routine because the other routines are of minor interest for the heat transfer measurement. This function averages over ten ADC values in a first step, then this average is corrected because the minimum current of the XTR105PA is not zero. In the last step the conversion from ADC value to degree celsius value is done and the result stored in an array for easy

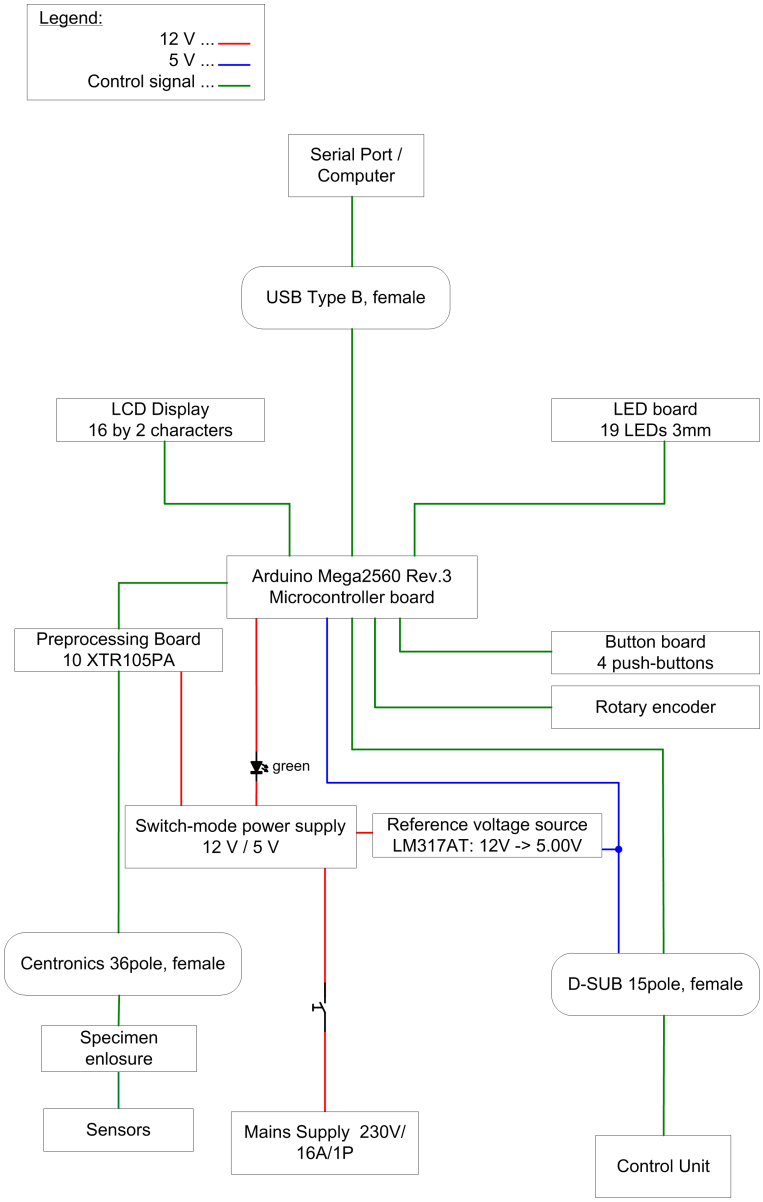

Figure 13: Block schematic of DAQ Unit

read-out later on.

Another routine handles the data transmission and formatting via the serial connection. The data is transmitted as a row of values separated by a # symbol starting with a time stamp created from the microcontroller runtime in milliseconds.

7.3.2 Matlab Code

The first section of code deals with configuration variable definition, specification data read in from a file and collecting workspace data for file handling. A background function manages the logging of all command window output ($\hat{=}$ shell output) to a log directory in the data storage directory. A graphical user interface (GUI) is initialized which offers four options: Serial streaming for a measurement, serial streaming test run with 100 datasets, read-in from a data file and run summary analysis.

Serial streaming for a measurement starts a measurement with a fixed value of 50 energy meter pulses. Afterwards a time stamp is created, a serial connection opened, the measurement started and a dialog box created showing the progress. Data is collected until the specified energy pulse count is reached. At last the collected data is read into a matrix B and formatted for subsequent calculations.

The serial streaming test run option executes the same steps as the serial streaming for a measurement routine with a different exit condition: data is collected until a hundred data sets have been read. The data file is marked with $-testrun-$ and excluded from automated data read-in. The third option of the GUI reads a selected data file into a matrix B and formats the matrix as needed for further computation.

After the data is correctly formatted in a matrix the time stamp is normalized and the characteristic deviation of each sensor is corrected. Following this steps the ADC noise is decreased by a smoothing function saving the data into matrix $B1$ for plotting.

The measurement time for the calculation of heat conductivity is determined within the given data by detecting the first and the last energy meter pulse. Calculating the mean values of the B values within this measurement time window and reading specimen specification data into variables follows. The next steps are calculations concerning the heat flux Q and testing for corrupted data. Q is deter-

mined by subtracting the heat losses at the flanges (multiplied with a coefficient for systemic losses) from the heat energy counted during the measurement time window.

In the last block a report with two pages is created and is saved as a PDF file. On the first page a sketch of the specimen shows average temperature values, results for $\lambda, \Phi, P_{heating}$ and the specimen specifications. The second page presents four plots showing the raw and smoothened data with and without the energy meter readings. If lambda calculation was successfully executed the mean values together with data file name and lambda calculation results are written to a special log file called $Run_Summary.csv$.

The last option shown in the graphical user interface manages the run summary read-out. Two choices are available: generate individual reports for all specimens and create an overview plot for all available data sets in the run summary list. Or define a specific specimen and generate the corresponding overview report for the selected sample. The resulting PDF files are stored in the data storage directory given by the configuration variables. Reports for the individual samples show: a distribution plot of all data sets meeting the data quality criteria set in the run summary function file, mean lambda value of those data sets, standard deviation for this value and the specification data for the specimen.

7.3.3 Finite element model

A three dimensional and an axis-symmetric two dimensional model for a finite element simulation was created to determine the heat losses through the flanges. Due to the convection calculation results in section 5.3.1 a natural convection mechanism combined with heat transfer in solids was chosen. The heat flux into and out of the flanges was gained by surface integration. Fig.14b shows the significant heat flux decrease with a rubber ring covering the surface area otherwise left uninsulated (see Fig.14). The reduced heat loss is indicated by the brighter colors in the area inside of the ring (see Fig.14b).

More detailed geometric models for each of the used pipe types were used to generate the corresponding heat flux data sets for the lambda calculation. The resulting temperature distributions are shown in Fig.15a-c.

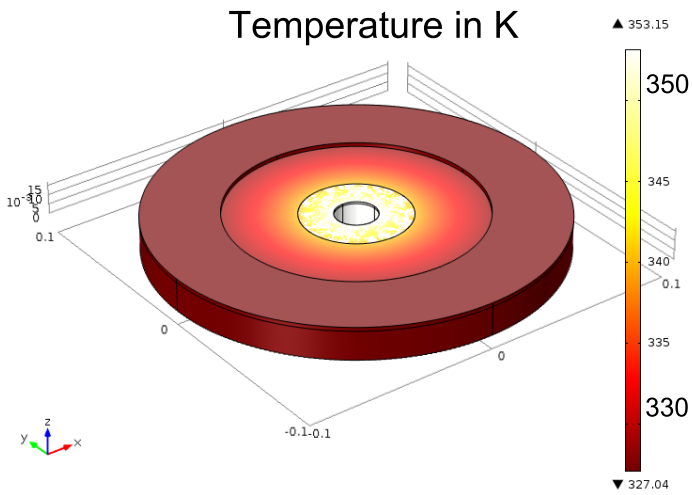

(a) Temperature distribution of flange B

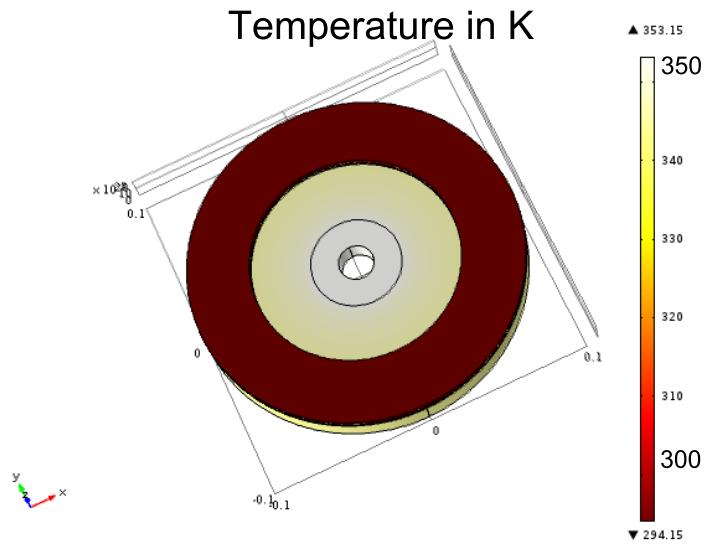

(b) Temperature distribution of flange B with an added rubber insulation

Figure 14: COMSOL Multiphysics 3D model of heat transfer in the flanges

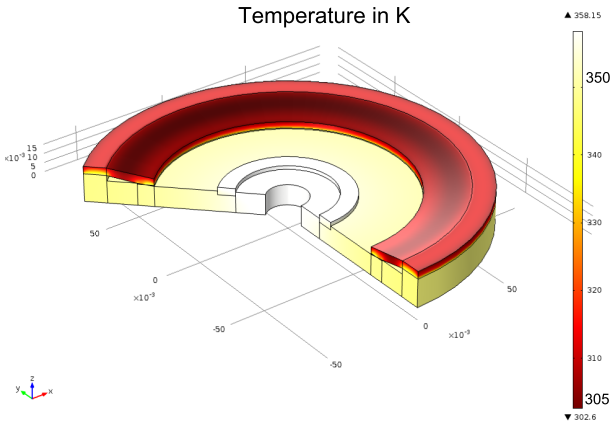

(a) Flange DN50-125

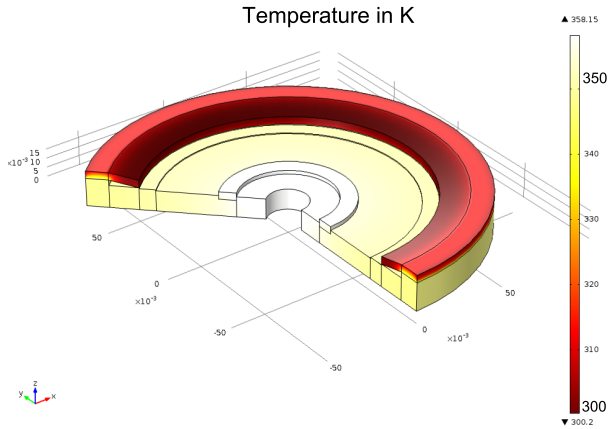

(b) Flange DN50-140

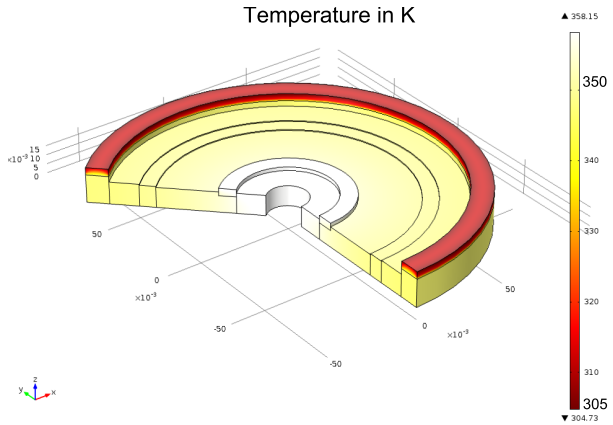

(c) Flange DN50-160

Figure 15: COMSOL Multiphysics 3D models of heat transfer in the altered flanges

8 Measurements

Thanks to the contributions of project partners a well chosen sample was devised which is presented in Tab.1 together with the corresponding measurement results. The deviations of the collected data sets can be described by a Gaussian distribution. Therefore, the given range of $\pm 1\sigma_{mean}$ around the mean value include 68.27 % of all possible values (according to general probability calculations).

Table 1: Specimen Overview

Nr.	ID	Size	Age $[years]$	λ_{mean} $[W/m \cdot K]$	σ_{mean} [%]
1	isop.ref1	DN50 / 125	0 (new product)	0,0246	6,9
2	isop.ref2	DN50 / 125	0 (new product)	0,0269 [a]	6,3
3	linz.kel1	DN50 / 125	0 (new product)	0,0230	9,7
4	linz.kel2	DN50 / 125	0 (new product)	0,0259	4,6
5	isop.alt1	DN50 / 125	5 (in storage)	0,0271	5,1
6	isop.alt2	DN50 / 125	5 (in storage)	0,0239	7,4
7	sten.iso1	DN50 / 140	24 (used at 80°C)	0,0295	3,6
8	isop.ref5	DN50 / 140	0 (new product)	0,0269 [a]	4,8
9	enag.pvc1	DN50 / 160	35 (used at 90°C)	0,0289	4,5
10	isop.ref6	DN50 / 160	0 (new product)	0,0265 [a]	4,0

[a] Calibration specimen

The first group of specimens (Tab.1 Nr.1 to 6) are unused compound pipes fulfilling current standards which were produced only weeks before testing. The next group are unused pipes (Tab.1 Nr.7 to 8) with a production date in the year 2007 to investigate the aging process under storage conditions. The last group of specimens (Tab.1 Nr.9 to 10) consists of two pipes after long-term operation and unused counterparts for referencing purposes.

Used and unused specimens were tested in order to answer the key questions of changing heat conductivity for closed cell foam PUR insulation materials. The measurement setup was designed for complete compound pipe sections to minimize the risk of damaging the test pieces due to complicated specimen preparation. Possible consequences of extensive preparation could include: loss of structural integrity of the foam layer caused by mechanical stress. Distortion of the results due to wrong assumptions concerning boundary layers and foam defects.

To reach the desired data quality of the results several factors have to be considered. On the one hand statistical fluctuations are compensated by taking the average value of lambda for multiple measurements. A more detailed description of this part of the calculations is shown in Section 8.2. On the other hand deviations due to system characteristics (e.g. differences between idealistic computer model and real system) need to be addressed. The solutions of the heat conductivity equations for the flanges have a strong influence on the calculation of lambda. Therefore, a reference specimen is used to determine this offset. In Section 8.1 this measurements are described in more detail.

The standard procedure for measuring a specimen did include the following steps:

- Grind, deburr and clean specimen ends.
- Measure and write documentation of pipe diameters and length.
- Label the specimen, mount sensors and flanges.
- Fill pipe with fluid and mount heating element.
- Test for leaks and mount assembly in specimen housing.
- Heat up specimen until thermal equilibrium is reached.
- Execute 10 measurements and create a report for each run.
- Create measurement report for each specimen.

8.1 Reference Measurements

A reference measurement was conducted in order to minimize deviations between the individual ADC channels combined with the read out circuit connecting it to the sensor elements. A set of Pt100 sensors (one sensor for each DAQ input channel) together with a calibrated temperature probe were fixed onto an aluminium block (see Fig.16). In submerging the greater part of the metal body into an ice water bath the necessary homogeneous temperature distribution at the mounting surface of the sensors was achieved. The sensors were insulated against the ambient air temperature by adding a strip of closed cell plastic foam to increase temperature homogeneity even further. There are only minor differences between channels as shown in Fig.17 for a similar setup where all sensors were at the same thermal level. The absolute differences are eliminated by using offset values in the analysis software configuration. To reduce the relative fluctuations of each channel an algorithm for ADC noise removal is integrated in the data filtering routine.

Figure 16: Sensor calibration in ice bath

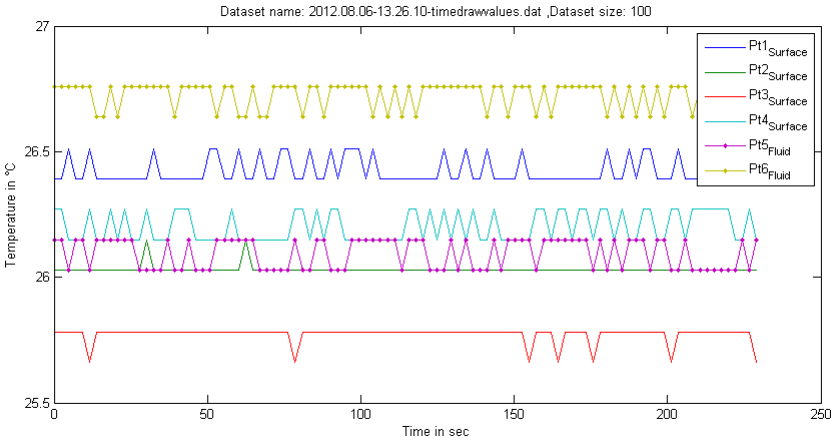

Figure 17: ADC channel deviation

8.2 Deviations & Reproducibility

The heat losses through the flanges are calculated aided by a two dimensional computer simulation of an idealized model. Therefore, reference specimens with a known heat conductivity were measured and, utilizing this data, compensation factors for the simulation solutions were calculated.

To prove the reproducibility of measurements a second reference specimen was tested and repeated measurements showed only small deviations. To validate the used computer model and the referencing method a validation specimen with the same properties as the reference sample was tested. The resulting data is compared in Fig.18. The difference of the shown mean values for specimens isop_ref6 and isop_ref7 (reference sample) of $\approx 4.5\,\%$ is within an acceptable range.

In Fig.19a a slightly stronger mean fluctuation in the first measurement run of each runtime can be seen (mean value marked with green line). After calculating the impact of this aberration on the results this effect is neglected due to insignificant influence.

The relative deviation from the mean value per measurement series and for multiple runs are shown in Fig.19b. No significant drift across multiple measurement series

was detected: the order of magnitude of these histograms ($1 \times 10^{-3}\,\mathrm{W/(m\,K)}$ to $1 \times 10^{-4}\,\mathrm{W/(m\,K)}$) is small. The distribution is similar to a discrete uniform distribution. Therefore, relative result deviation seems to be random.

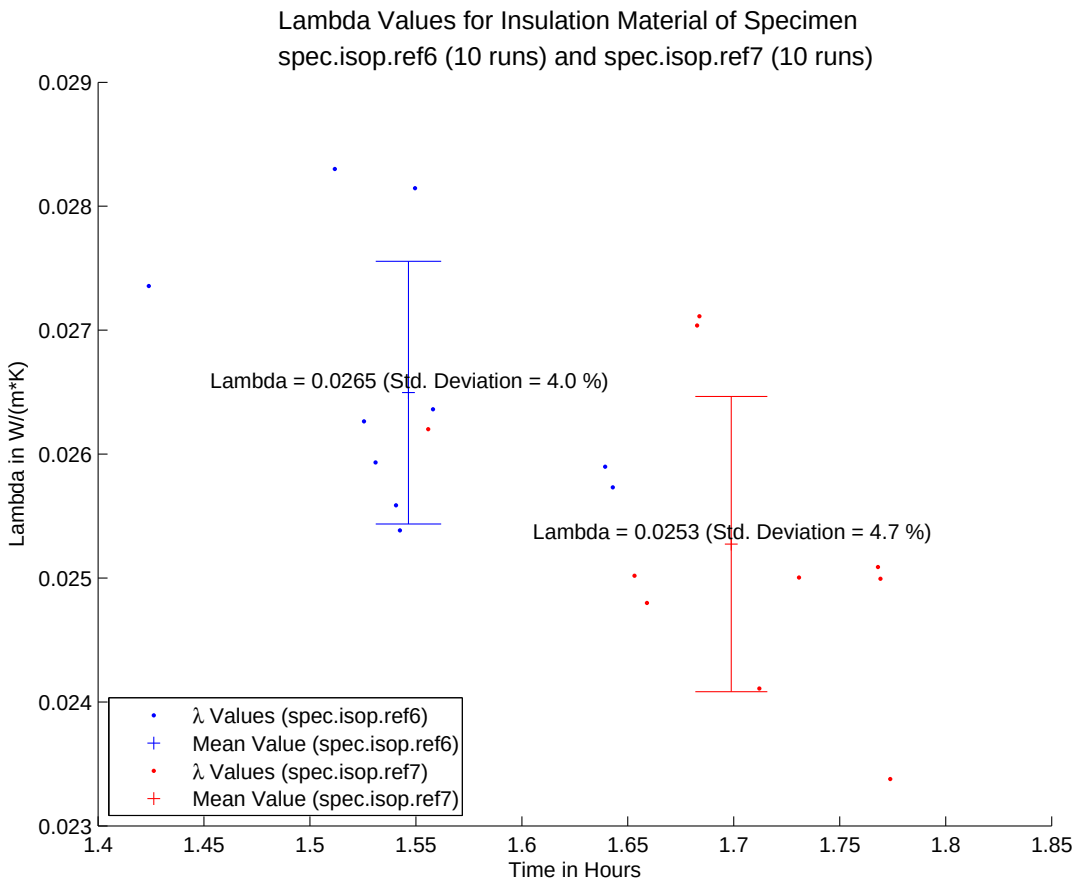

Figure 18: Plot of a reference and validation specimen

8.3 Result Overview

The results of all measurements are depicted in Fig.20. For easier separation of the different specimen classes the error bars are color coded: Green for new samples, orange for unused specimens after prolonged storage and red for specimens after more than 20 years of usage. The age in years of each specimen tested is presented in the legend at the lower right corner of Fig.20.

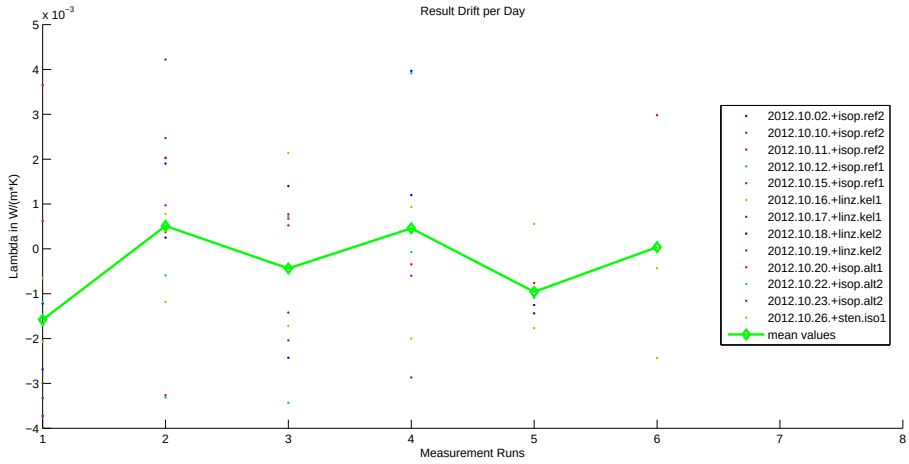

(a) Drift per day

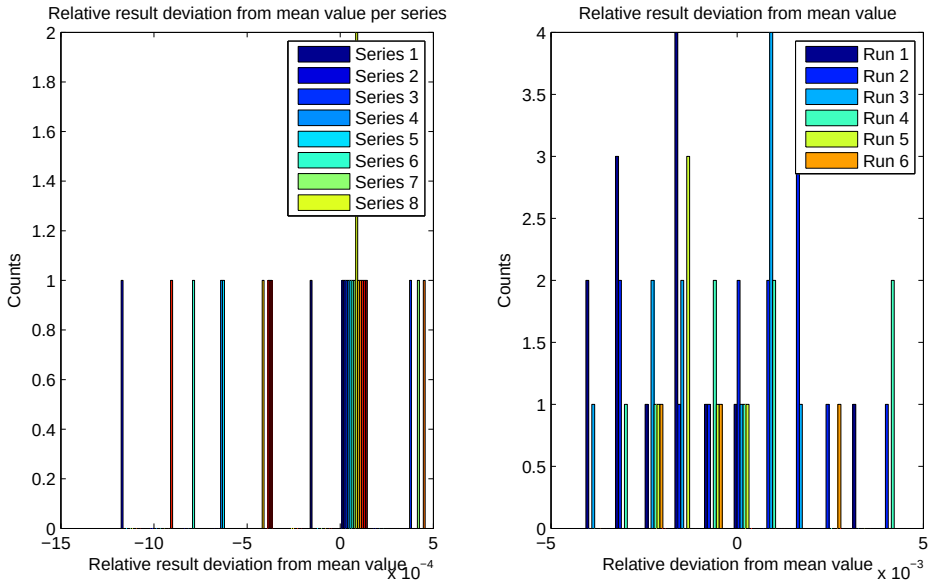

(b) Drift per series and run

Figure 19: Result Drift

8.4 Interpretation

The gained data confirms the tendencies discovered by previous studies concerning the aging effects on thermal conductibility of plastic jacket pipes used in district heating systems. However, in this study several interesting observations were

made regarding the measurement results. The first four specimens (isop_ref1, isop_ref2, linz_kel1, linz_kel2) are unused DN 50/125 pipes directly taken from two different producers. They show a similar scattering with mean values of $\lambda \approx 0.0258\,\mathrm{W/(m\,K)}$, $\Delta\lambda \lesssim 9\,\%$ and $\lambda \approx 0.0245\,\mathrm{W/(m\,K)}$, $\Delta\lambda \lesssim 12\,\%$. Their absolute mean values for the heat conductibility λ are within and below the upper limit of $\lambda \leq 0.0270\,\mathrm{W/(m\,K)}$ defined by the producing companies. Moreover, they are well below the upper limit of $\lambda \leq 0.0290\,\mathrm{W/(m\,K)}$ governed by the European standard EN 253 [8, p.18] for new pipes.

The next two specimens (isop_alt1, isop_alt2) are unused pipes after 5 years of storage. They show no significant change compared to the first four samples and confirm the product stability concerning the effect of prolonged storage on λ.

Although the duration of operation for sample enag_pvc1 amounts to 35 years its relative increase in λ of $\lesssim 9\,\%$ is smaller than the relative increase of $\lesssim 10\,\%$ for specimen sten_iso1 with 24 years. This result can be explained by the different insulation thickness, sten_iso1 is sized DN 50/140 whereas the other one is sized DN 50/160. Therefore, this leads to the deduction that larger insulation layer thickness decelerates overall thermal ageing. An other conclusion of these last four measurement results is: even after prolonged usage at conventional operation temperatures in the range of 80 °C to 90 °C only small relative increases in λ of $\lesssim 10\,\%$ were detected. This result is significantly smaller than anticipated based on former studies but it is in accordance with the findings of another recent study [7, p.84ff].

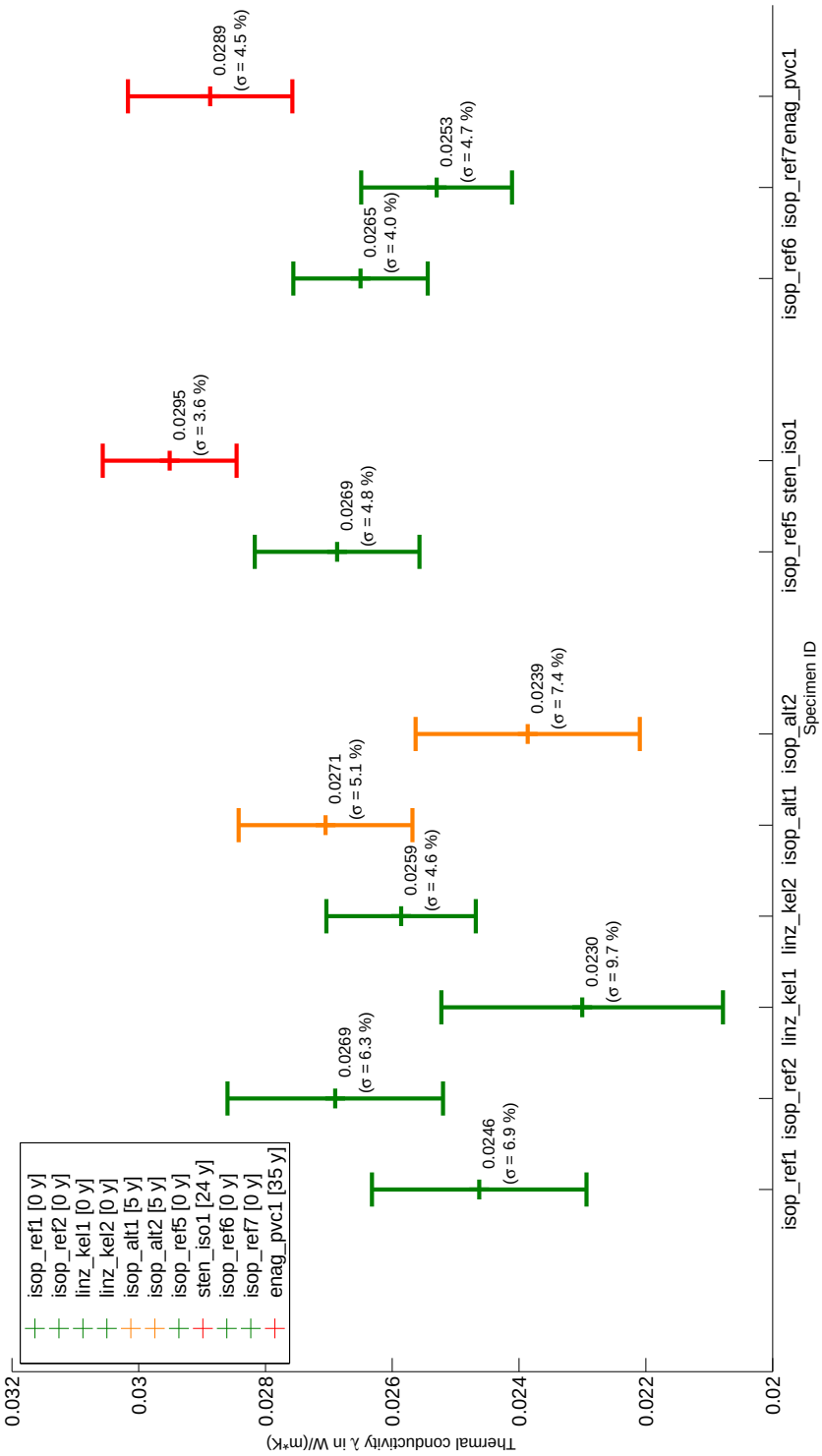

Figure 20: Result Overview

9 Conclusion

Both main objectives of this study are fulfilled: on the one hand a cost efficient and reliable measurement system to determine the thermal conductivity of insulation layers in compound pipes was developed. On the other hand unused and used plastic jacket pipes in various states were measured to study the change of thermal conductivity due to aging effects in the insulation material for PUR closed-cell foams.

A well designed system was devised to maximize measurement accuracy and ease of operation. The samples can be changed easily and require minimal preparation effort in advance. A balanced combination of hard- and software components as well as computer simulations save man hours and energy consumption. The samples are mounted on two support holders in a temperature controlled environment. A control unit regulates the heating and cooling elements. A data acquisition unit converts the electric sensor signals into a digital data stream accessible via a virtual serial port. The samples are filled with a fluid and heated by a central heating rod. Temperature sensors on the surface and within the pipe combined with geometric specimen dimensions and known material properties permit the calculation of the thermal conductivity. Finite element models were used to determine the influence on the calculations and magnitude of convection, thermal radiation and heat flux.

The gained data confirms general trends of previous studies concerning the aging effects on thermal conductivity of plastic jacket pipes used in district heating systems. However, the results implicate less deterioration of the insulating properties than former publications stated. Thermal conduction measured for unused pipes is within and below the upper limit of $0.0270\,\mathrm{W/(m\,K)}$ defined by the producing companies and well below the upper limit of $0.0290\,\mathrm{W/(m\,K)}$ governed by the European standard EN 253 for new pipes.

Unused pipes after 5 years of storage show similar values thus confirming the product stability concerning the effect of prolonged storage on the thermal conductivity. The used sample pipes showed that even after prolonged operation

of more than 20 years at usual temperatures in the range of 80 °C to 90 °C only small relative increases in thermal conductivity smaller than 10 % can be detected.

Measurement data from this study indicate less strong aging effects than anticipated. Therefore, further investigation in this field and a larger set of samples is advisable.

List of Figures

1 Plastic jacket pipe cross sections (DN50/160) 7
2 Schematic cross section of a DN 50-125 plastic jacket pipe 12
3 Plots concerning the heat transfer coefficient α 14
4 Simulation data of flow distribution in a compound pipe 16
5 Simulation data of temperature distribution in a compound pipe . . 17
6 Technical drawing of Flange A 21
7 Stainless steel bands for sensor mounting 22
8 Specimen housing 23
9 Specimen enclosure top view with mounted sample 24
10 Finished Control Unit 25
11 Block schematic of Control Unit 26
12 Finished Data Acquisition Unit 28
13 Block schematic of DAQ Unit 30
14 COMSOL Multiphysics 3D model of heat transfer in the flanges . . 34
15 COMSOL Multiphysics 3D models of heat transfer in the altered flanges 35
16 Sensor calibration in ice bath 38
17 ADC channel deviation 39
18 Plot of a reference and validation specimen 40
19 Result Drift 41
20 Result Overview 43

10 References

[1] Harwell AEA. *Green Public Procurement - Thermal Insulation Technical Background Report*. European Commission, 2010.

[2] T.E. Diller. Advances in heat flux measurement. In *Advances in Heat Transfer*, pages 279–368. Boston: Academic Press, 1993.

[3] XCO2 Conisbee Ltd. Consulting Engineers. *Insulation for Sustainability - A Guide*. XCO2 Conisbee Ltd. Consulting Engineers, 2002.

[4] GEF Ingieursgesellschaft für Energietechnik und Fernwärme Chemnitz GmbH; IMA Materialforschungs-und Anwendungstechnik GmbH; IPF Leibnitz-Institut für Polymerforschung Dresden e.V. *Zeitstandfestigkeit von Kunststoffmantelrohren - Permeations- und Degradationsverhalten, Wechselbeanspruchung, Alterungsgradient, Muffenbewertung, Versagensverhalten.* GEF; IMA; IPF, 2011.

[5] Deutsches Institut für Normung e.V. *Rohre aus unlegiertem Stahl mit Eignung zum Schweißen und Gewindeschneiden - Technische Lieferbedingungen.* Deutsches Institut für Normung e.V., 2010.

[6] Verein Deutscher Ingenieure. *VDI Heat Atlas.* Springer-Verlag Berlin Heidelberg, 2 edition, 2010.

[7] Verein Deutscher Ingenieure. *VDI Heat Atlas.* Springer-Verlag Berlin Heidelberg, 2 edition, 2010.

[8] Austrian Standards Institute. *Fernwärmerohre - Werkmäßig gedämmte Verbundmantelrohrsysteme für direkt erdverlegte Fernwärmenetze.* Austrian Standards Institute, 2009.

[9] M.K. Mukhopadhyaya, P.; Kumaran. Long-term thermal resistance of closed-cell foam insulation. In *3rd Global Insulation Conference and Exhibition*, 2008.

[10] Dr.-Ing. Winfried Schuricht. *Alterung von Kunststoffmantelrohren.* Dresdner Fernwärme-Kolloquium, 2004.

[11] Baehr Stephan. *Wärme- und Stoffübertragung.* Springer-Verlag Berlin Heidelberg, 7 edition, 2012.

[12] ThyssenKrupp. *Werkstoffblatt TK 1.4301.* ThyssenKrupp Materials Europe GmbH, 2006.

[13] Y.I. Cho W.M. Rohsenow, J.P. Harnett, editor. *Handbook of Heat Transfer.* McGraw-Hill Companies, 3 edition, 1998.